Armeniaspirols inhibit the ATP-dependent proteases ClpYQ and ClpXP in Gram-positive bacteria, dysregulating the divisome

Puneet Labana,[1] Mark H. Dornan,[1] Matthew Lafrenière,[1] Tomasz L. Czarny,[2] Eric D. Brown,[2] John P. Pezacki,[1] Christopher N. Boddy[1]*

[1]Department of Chemistry & Biomolecular Sciences, University of Ottawa, Ottawa, ON K1N 6N5
[2]Department of Biochemistry & Biomedical Sciences, McMaster University, Hamilton, ON L8S 4L8

Abstract

The emergence of multi-drug resistant organisms clinically presents major challenges to managing human health and threaten the great progress that has been made in preventing morbidity in the age of antibiotics. In order to combat these pathogens, new antibiotics with diverse mechanisms of action will be required. Armeniaspirols represent a novel class of natural product-based antibiotic molecules with unknown mechanisms of action. Herein, we synthesized analogs of armeniaspirol and studied their antibiotic properties and mechanism of action. Using a combination of chemoproteomics, quantitative proteomics, and a battery of functional assays we discovered that armeniaspirols inhibit the bacterial divisome through direct inhibition of the ClpYQ and ClpXP proteases. This was validated by comparisons with genetic knockouts. Sub-lethal challenges suggested that resistance to armeniaspirol inhibition of ClpYQ and ClpXP proteases was difficult to achieve without catastrophic consequences for the bacteria. Thus, the armeniaspirols represent an important new tool to combat multi-drug resistance, through a potent and highly novel mechanism of action.

Introduction

Since the discovery of penicillin by Sir Alexander Fleming in 1928 that marked the beginning of the age of antibiotics, human morbidity has dramatically improved and countless pandemics avoided. Millions of lives are saved per year through the use of antibiotics, not to mention the countless successes in treating non-life-threatening opportunistic infections. In the US alone, over 250 million prescriptions for antibiotics are prescribed per year[1]. Threatening this progress is the global emergence of multi-drug resistant bacterial pathogens that continue to increase in number and represent a looming public health crisis that threatens one of the underpinnings of modern medicine, namely effective antibiotic therapies.

The vast majority of clinical antibiotics are derived from natural products and target either the bacterial cell wall, ribosomes, or DNA[2]. These similar mechanistic targets enable high-level multi-drug

resistance mechanisms to be readily transferred between bacteria. An increasing number of pathogens are becoming resistant to many, sometimes all, of our clinical antibiotics and few new antibiotics effective against these resistant pathogens are in development. Thus, identification and development of antibiotics that interact with new biochemical targets will be an integral part of the solution to combating antimicrobial resistance. New antibiotics, like teixobactin[3], for which resistant bacteria strains cannot readily emerge are rare and of significant interest. The natural product armeniaspirol A distinguishes itself as a potent and promising example of these.

Armeniaspirols A-C that were isolated from *Streptomyces armeniacus* DSM19369[4] in 2012 represent a new class of natural product-based antibiotic with an unknown mechanism of action. These structurally unprecedented compounds (Fig. 1) are active against multidrug-resistant Gram-positive bacteria including methicillin-resistant *Staphylococcus aureus* (MRSA), vancomycin-resistant *Enterococcus* (VRE) and penicillin-resistant *Streptococcus pneumoniae* (PRSP) at low micromolar concentrations[4,5] (Supplementary Table 1). Armeniaspirol A is active against MRSA in an *in vivo* sepsis model, and *in vitro* resistant *S. aureus* strains could not be generated even after 30 serial passages under sub-lethal doses[4].

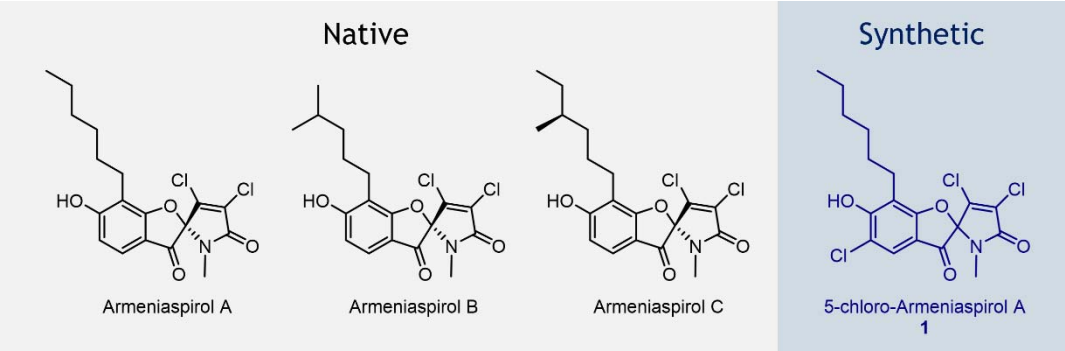

Figure 1. Structures of armeniaspirols A – C. Armeniaspirols were isolated from *Streptomyces armeniacus* DSM19369 and possess a unique spiro-[4.4]non-8-ene scaffold. A synthetic route to armeniaspirol A generated the chlorinated derivative 5-chloro-armeniaspirol A, **1**.

Herein we use a combination of quantitative proteomics, inhibitor covalent capture, biochemical characterization, and microscopy to show that armeniaspirol directly inhibits both the ClpYQ and ClpXP proteases in *Bacillus subtilis*. Inhibition of these proteases disrupts the divisome function and is responsible for the antibiotic activity of armeniaspirol. Armeniaspirol represents a new class of inhibitor for members of the AAA+ family of proteolytic machines, which includes ClpYQ and

ClpXP in addition to the 20S and 26S proteasomes[6]. The multiple targets and complex pleotropic effects observed from armeniaspirol treatment likely contribute to the ability to kill Gram-positive bacteria without detectable resistance.

Results

Armeniaspirol does not interact with common antibiotic targets

In order to probe the mechanism of action of armeniaspirol, we used dimethyl isotopic labelling[7] to quantitatively profile changes to the bacterial proteome upon treatment with sub-lethal levels of chloro-armeniaspirol, **1** (Fig. 2a,b). **1** was obtained by chemical synthesis (Supplementary Scheme 1) and has comparable activity to armeniaspirol A against *B. subtilis*[5]. *B. subtilis* is one of the best studied Gram-positive bacteria[8] and serves as a useful model organism for Gram-positive pathogens, including *S. aureus*. Given that its proteome has been extensively profiled in response to a number of antibiotic classes[9–14], we profiled the impact of 1 μg/mL of **1** (2.4 μM) on *B. subtilis* representing ½ the minimum inhibitory concentration (MIC).

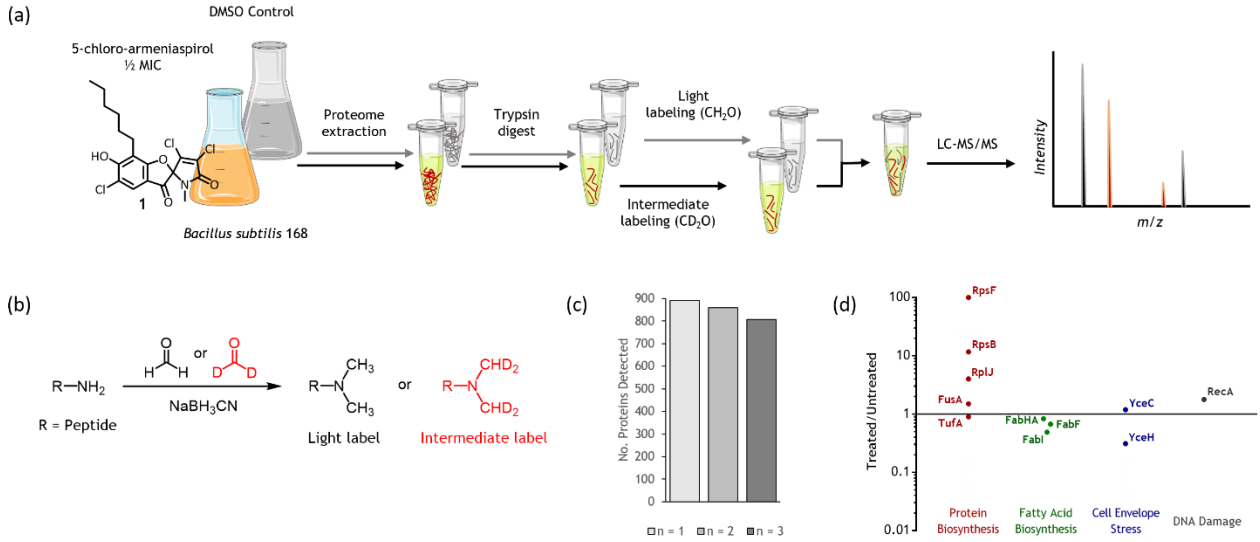

Figure 2. Dimethyl labeling of the *B. subtilis* proteome and quantitative proteomics. (a) Proteome extract of *B. subtilis* 168 following 1- and vehicle control- treated growth are isotopically labeled with formaldehyde and deuterated formaldehyde, respectively. Compound 1 treated growth conditions are shown in colour, while vehicle control treated growth conditions are shown in grey. Experiments were carried out in biological triplicate (n=3). (b) Stable isotope dimethyl labeling by addition of formaldehyde at the N-terminus and ε-amino groups of lysine residues, followed by the immediate reduction with sodium cyanoborohydride. (c) Total protein recovery following dimethyl labeling, shown for each replicate. (d) Characteristic upregulated protein markers of various antibiotic treatments. No significant overlap is observed with armeniaspirol treatment (geometric means of triplicate data plotted for each protein; exception YceH which was detected in 2 of 3 replicates). See Supplemental Dataset 1.

Comparing the proteome from *B. subtilis* cultures treated with **1** to literature data for *B. subtilis* cultures treated with a variety of antibiotics with known mechanisms depicts a unique fingerprint. This includes the proteomes from *B. subtilis* treated with antibiotics that inhibit protein synthesis (tetracycline and chelocardin)[10], fatty acid biosynthesis (platencin, platensimycin, cerulenin and triclosan)[11], cell wall biosynthesis (merscadin, bacitracin, and vancomycin)[12], and those that act as DNA damaging agents (mitomycin, daunomycin, and adriamycin)[9,14] (Fig. 2d; see Supplementary Table 2 for detailed comparison). Using checkerboard assays to identify interactions within common pathways targeted by antibiotic, **1** was shown to function independently of tetracycline, cerulenin, the cell wall biosynthesis inhibitor penicillin, and the DNA replication inhibitor ciprofloxacin (all FIC indexes >0.5; see Supplementary Table 3). Taken together, these data suggest that armeniaspirol does not interact with any of these common antibiotic targets.

Novel target discovery by inhibitor covalent capture

We thus took advantage of armeniaspirol's electrophilic nature to covalently capture direct biochemical targets from the *B. subtilis* proteome. Several derivatives of **1** were synthesized and assayed for their MICs, enabling us to draw key structure activity relationships (Fig. 3a; Supplementary Scheme 1). MIC data clearly shows the free phenol is critical for retaining activity, while extending the N-alkyl chain significantly increased the compound's potency. Based on these results we installed a biorthogonal reactive group containing an alkyne to facilitate target capture in place of the N-methyl of armeniaspirol, generating probe **2** (Fig. 3b; Supplementary Scheme 1). Gratifyingly this compound retained activity with an MIC of 8 μg/mL (13.4 μM) against *B. subtilis*.

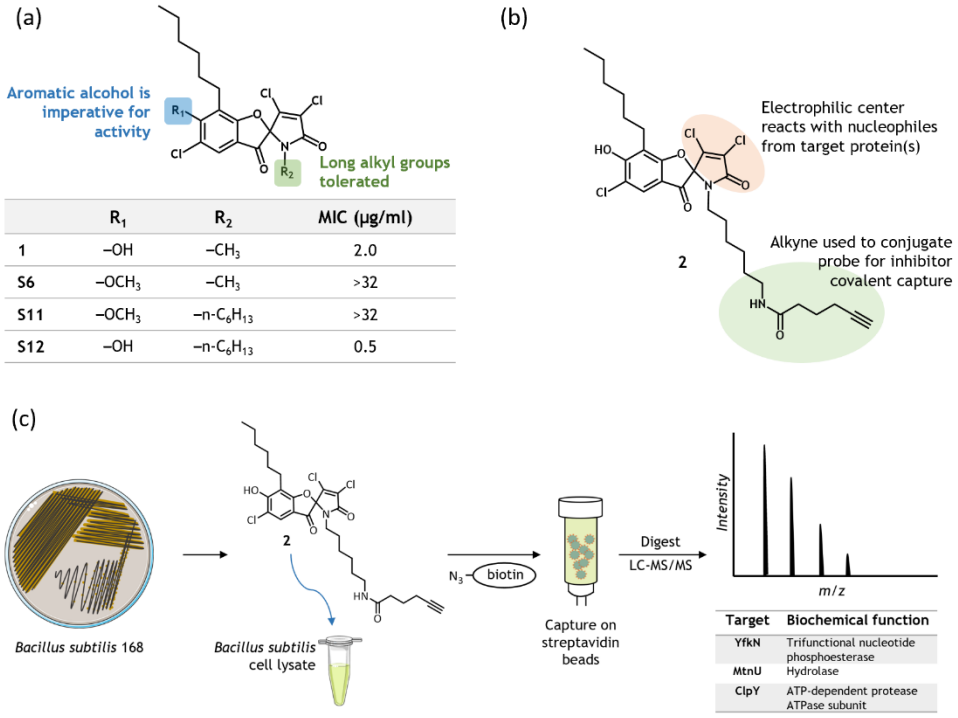

	R_1	R_2	MIC (μg/ml)
1	–OH	$–CH_3$	2.0
S6	$–OCH_3$	$–CH_3$	>32
S11	$–OCH_3$	$–n\text{-}C_6H_{13}$	>32
S12	–OH	$–n\text{-}C_6H_{13}$	0.5

Target	Biochemical function
YfkN	Trifunctional nucleotide phosphoesterase
MtnU	Hydrolase
ClpY	ATP-dependent protease ATPase subunit

Figure 3. Inhibitor covalent capture strategy for identifying the direct biochemical targets of armeniaspirol. (a) Structure-activity relationship for armeniaspirol antibiotic activity. (b) Armeniaspirol-derived covalent capture probe, 2. (c) Experimental workflow for identifying targets of armeniaspirol. The electrophilic center binds to the protein of interest in *B. subtilis* 168 cell lysate. The free alkyne is conjugated to biotin-azide and captured on streptavidin beads. Captured proteins are subjected to digestion and LC-MS/MS for identification. Three potential candidates were obtained: YfkN, MtnU, and ClpY.

Our target capture strategy involved treatment of *B. subtilis* cell lysate with **2** to pull down all candidate targets. To discern potential targets from false positives, cell lysate was pretreated with **1** in competition assay to block binding sites on potential targets, and subsequently treated with **2** to capture only non-selective false positive interactions. All captured proteins were recovered by crosslinking the probe with biotin-azide and capturing the probe with its associated proteins onto streptavidin beads. On-bead digestion followed by LC-MS/MS target identification identified three candidates whose abundances were blocked by addition of **1**: YfkN, MtnU and ClpY (Fig. 3c; also see Supplementary Table 4).

YfkN and MtnU are not direct biochemical targets of armeniaspirol

YfkN, a trifunctional nucleotide phosphoesterase, is the largest protein synthesized in *B. subtilis* and the only essential protein of the three targets identified[15,16]. A CRISPR interference (CRISPRi) strategy[17] was applied to knockdown *yfkN* levels in *B. subtilis*, and this strain was tested for

armeniaspirol sensitivity by a MIC assay. If armeniaspirol directly binds and inhibits YfkN, we would expect greater sensitivity to **1** in the knockdown strain than in the wild-type strain. However, the knockdown strain and wild-type exhibited identical sensitivities to **1** with MICs of 2 µg/mL (4.8 µM; Supplementary Fig. 1a). This result is consistent with YfkN not playing a direct biochemical role in armeniaspirol's antibiotic activity.

MtnU is a non-essential protein linked to the methionine salvage pathway in *B. subtilis* but possesses an undefined biochemical role in the pathway[18]. To test the role of MtnU in armeniaspirol activity we determined the sensitivity of **1** to the *mtnU* knockout strain MGNA-A784 (*mtnU::erm*)[19]. If MtnU is the direct target of armeniaspirol, the knockout strain should be insensitive to **1**. The MIC of **1** for MGNA-A784 was 2 µg/mL (4.8 µM). As this is identical to the wild-type strain, MtnU is not responsible for the antibiotic activity of armeniaspirol (Supplementary Fig. 1b).

ClpYQ and ClpXP ATP-dependent proteases are targets of armeniaspirol

ClpY is the ATPase component of the ATP-dependent ClpYQ protease in *Bacillus subtilis*[20] (also known as HslVU and CodWX). ClpY forms two stacked hexameric rings[21] that recognize and unfold native protein substrates[22]. The unfolded proteins are translocated into the catalytic chamber of the associated protease[22], ClpQ, which also forms two stacked hexameric rings[23] and performs proteolysis through an N-terminal active site serine[20]. In general, bacterial ATP-dependent proteases maintain protein quality by degrading damaged and misfolded proteins and protein fragments[22]. In addition, they can play key roles in controlling cellular processes by degradation of regulatory proteins[22]. However, the role of ClpYQ in *B. subtilis* is poorly characterized[24].

As an *in vitro* activity assay for *B. subtilis* ClpYQ had previously been developed[20,25], we readily expressed and purified ClpQ (bsClpQ) and ClpY (bsClpY) and were able to kinetically quantify its proteolysis activity with the fluorogenic peptidic substrate, Cbz-GGL-AMC (Fig. 4a; Supplementary Fig. 2a). The addition of **1** shows dose-dependent inhibition of proteolysis with an IC_{50} of 15 ± 1 µM (Fig. 4b). Kinetic characterization of inhibition by **1** identified it as a reversible, competitive inhibitor of proteolysis with a K_i of 1.5 µM (Supplementary Fig. 2b,c,d).

Additionally, control experiments showed that ATPase activity is essential for proteolysis (Fig. 4a; Supplementary Fig. 2d). **1** inhibited the ATPase activity of bsClpYQ with an IC_{50} of 42 ± 1 µM (Fig. 4c). Based on these data, **1** is clearly an inhibitor of ClpYQ proteolysis and ATPase activity. However, **1** does not inhibit proteolysis by directly inhibiting the ATPase activity since there is significant ATPase activity

at concentrations of **1** where there is little to no protease activity. Our data are thus consistent with **1** directly interacting with the ATPase ClpY in the ClpYQ complex and allosterically regulating or decoupling ATPase and proteolytic function, although these data do not rigorously exclude **1** binding to ClpQ.

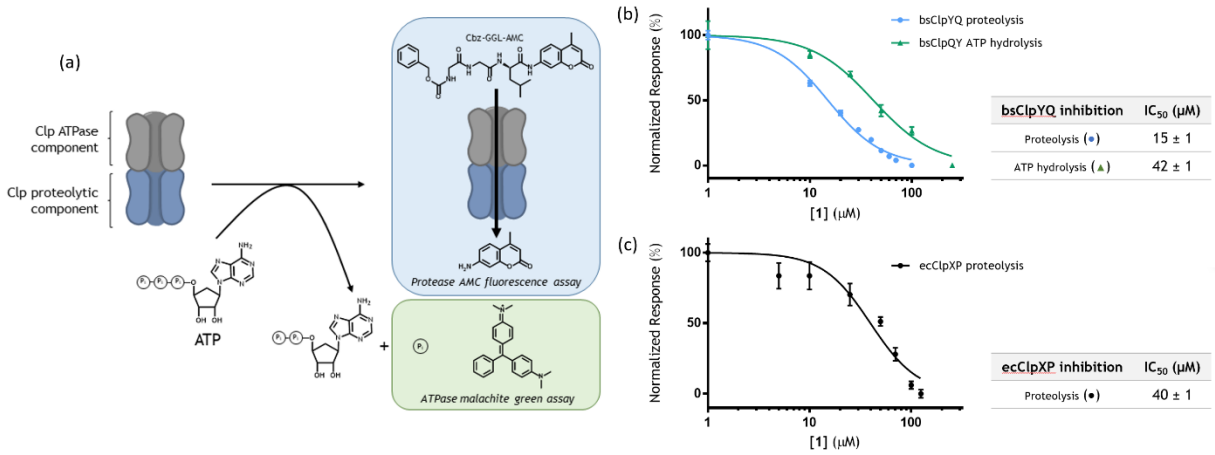

Figure 4. Inhibition of bsClpYQ and ecClpXP peptidase and ATPase activity by 1. (a) General schematic for the degradation of fluorogenic peptide, Z-GGL-AMC, leading to the release of AMC that can be detected at an excitation and emission of 355 nm and 460 nm, respectively. Alternatively, ATP hydrolysis is monitored by malachite green dye and free phosphorous is detected at 650 nm. (b) An IC50 of 15 μM was obtained with 0.1 mM Cbz-GGL-AMC substrate for bsClpYQ proteolysis, while an IC50 of 42 μM was obtained with 1 mM ATP for bsClpYQ ATPase. (c) An IC50 of 40 μM was obtained with 0.1 mM Suc-LY-AMC substrate for ecClpXP proteolysis. All data points were obtained in triplicate.

Surprisingly, both the Δ*clpQ* and Δ*clpY* individual deletion strains (BKE16150 [*clpQ::erm*][26] and MGNA-A086 [*clpY::erm*][19], respectively) were equally sensitive to **1** as shown by their MICs (Supplementary Fig. 1b). This result suggests a more complex mechanism of action with multiple biochemical targets. We thus sought to determine whether the related ClpXP protease[27] from *B. subtilis* (bsClpXP) was also inhibited by **1.** ClpXP is composed of a hexameric ring of the ATPase ClpX bound to a heptameric ring of the protease ClpP[27]. ClpXP binds to unstructured peptide tags in proteins, such as the ssrA tag appended to incomplete nascent proteins on stalled ribosomes[28,29] and a C-terminal tag on the essential cell division protein FtsZ[30,31,32], and targets these proteins for unfolding and proteolysis. Although we were able to express and purify bsClpXP, we could only achieve single turnover for proteolysis under all assay conditions investigated. We thus turned to *E. coli* ClpXP (ecClpXP), which has been previously characterized *in vitro*[33]. The amino acid sequences of ecClpX and bsClpX share 64% identity, while ecClpP and bsClpP share 70% identity. Our results showed **1** inhibited ecClpXP hydrolysis of Suc-LY-AMC *in vitro* with an IC_{50} of 40 ± 1 μM (Fig 4c).

To validate that armeniaspirol inhibits ClpYQ and ClpXP proteases in *B. subtilis*, we compared the effects of armeniaspirol treatment on the *B. subtilis* proteome to that of a *clpQ* and a *clpP* deletion mutant. Dimethyl isotopic labelling was used to quantitatively profile changes to the bacterial proteome of the Δ*clpQ* and Δ*clpP B. subtilis* knockout strains BKE16150 and BKK34540 (*clpP::kan*)[26], with wild-type *B. subtilis* 168 used as the control. Proteins that increased as compared to their controls by greater than 2-fold in two out of three biological replicates, with a geometric mean of all three replicates greater than 2, were considered to have increased (Fig. 5a). Treatment of **1** led to an increase in 369 proteins. The *ΔclpQ* and *ΔclpP* mutants showed 277 and 456 proteins increased, respectively. The 159 proteins that overlap between the armeniaspirol treatment and *ΔclpP* mutant and the 78 proteins that overlap between the armeniaspirol treatment and *ΔclpQ* mutant are a statistically significant increase over the expected values from random as determined by the Chi square goodness of fit test ($P < 0.0001$). This strongly supports our hypothesis that armeniaspirol is inhibiting the ClpYQ and ClpXP proteases in *B. subtilis*.

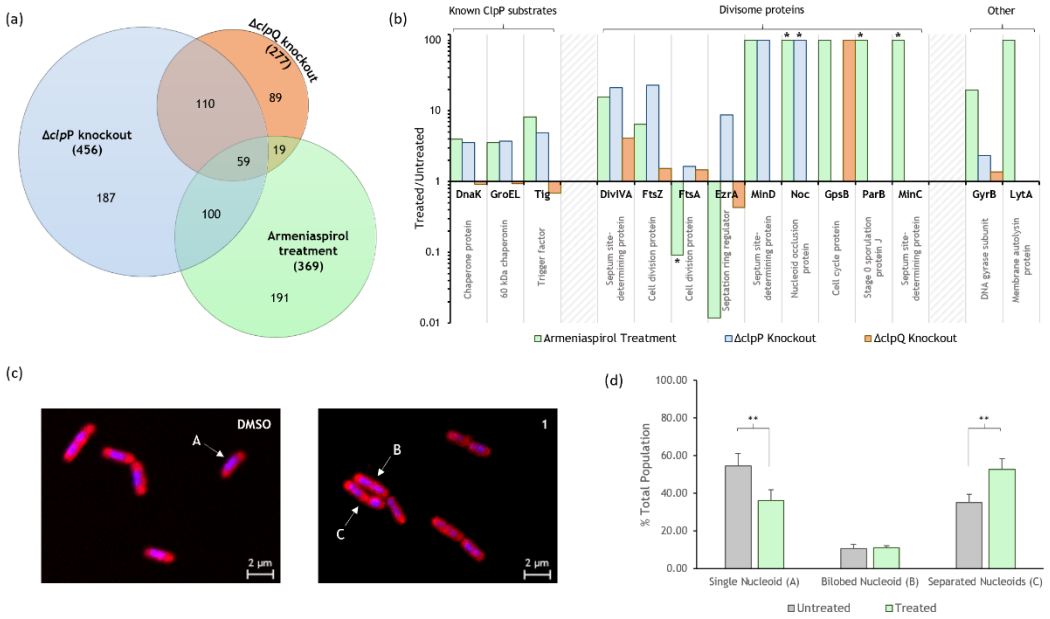

Figure 5. Implications of cell division inhibition in armeniaspirol-treated *B. subtilis* and *ΔclpP* and *ΔclpQ* mutants. (a) Venn diagram depicting upregulated proteins across *B. subtilis* 168 strains obtained from biological triplicates (n=3). (b) Effects on cell division protein abundances according to treatment (geometric means plotted; asterisks indicate proteins detected in only 1 of 3 replicates). (c) Micrographs of armeniaspirol-treated versus vehicle control treated *B. subtilis* showing representations of single nucleoids (A), bilobed nucleoids (B), and separated nucleoids (C). (d) Septation defect bar graphs, where cells were classified according to nucleoid phenotype (biological triplicate; Untreated n=149, Treated n=157). **$p < 0.05$, statistical analysis was performed by 2-way ANOVA with Holm-Sidak's multiple comparison test. See Supplemental Data set 2 and Supplemental Dataset 3 for Δ*clpP* and Δ*clpQ*

proteomic dataset respectively and Supplemental Dataset 4 for a list of all proteins that have increased in abundance.

While few substrates of the ClpYQ protease are known, a number of substrates of the ClpXP protease have been identified. For example, the highly abundant proteins DnaK, GroEL, and Tig are known ClpXP substrates[34,35,36,37,38]. All three show a significant increase in abundance in the Δ*clpP* strain and upon treatment with **1** (Fig 5b), which further supports inhibition of ClpXP activity by **1**.

Armeniaspirol dysregulates the B. subtilis divisome

To further identify how inhibition of the ClpYQ and ClpXP proteases by armeniaspirol impact *B. subtilis*, we examined the 369 proteins that increased in abundance upon treatment with **1**. Gene ontology (GO) analysis[39] identified GO terms associated with cellular metabolic processes being significantly overrepresented in this set (false discovery rate of 8.2×10^{-17}). This includes proteins responsible for Thr, Asp, Lys, His and β-branch amino acid biosynthesis as well as glycolytic processes. In addition, there was a significant overrepresentation in proteins with terms related to nucleotide scavenging, coenzyme metabolic processes, and organic acid metabolism. Because multiple bactericidal antibiotics including β-lactams, aminoglycosides, and quinolones have all been shown to increase the concentration of metabolites from these pathways in *E. coli*[40], the observed increase in protein levels for the enzyme responsible for their biosynthesis is likely not predictive of the direct biochemical target of **1**, but rather an indirect effect of antibiotic treatment.

Because both proteases play a role in housekeeping proteolysis, it is unlikely that their inhibition will lead to overrepresentation of a specific GO term. Similarly, targeted proteolysis by both proteases appears to be selective for specific proteins with regulatory function and thus is also unlikely to lead to overrepresentation of a specific GO term. Direct examination of the 369 proteins however identified a surprising trend. Several divisome proteins from *B. subtilis* showed an increase in abundance upon treatment with **1** (Fig. 5b).

The divisome plays an essential role during cell division. In *B. subtilis* cell division occurs at the midcell and is mediated by the formation of a ring-like structure on the inside of the plasma membrane via polymerization of FtsZ[41]. A number of additional proteins are recruited to the Z-ring, which facilitate constriction of the membrane and a directional change in peptidoglycan biosynthesis, ultimately leading to cytokinesis. Tight regulation of Z-ring formation with chromosome replication and segregation is maintained by two key negative regulators of cell division, the Min system, comprised of MinC and MinD which are involved in septum placement at the midcell[42], and the nucleoid occlusion system, principally

Noc, which prevents premature septation[43]. Key additional components of the divisome include the divisome proteins FtsA[44], ZapA[45], SepF[46], and EzrA[47], as well as the regulatory proteins GspB[48], DivIVA[48,49], and MinJ[50].

A number of these proteins, particularly the negative regulators of the cell divisome, increased in abundance upon treatment with **1** (Fig. 5b). Of all the known divisome related proteins[41] for which quantitative proteomic data was detected, only FtsA and EzrA did not show an increase in abundance. The Min system related proteins MinC, MinD, DivIVA, and GpsB, involved in negative regulation of cell division, all increased substantially (10-100 fold) as did the negative regulator Noc and its paralog ParB[51], which plays a similar role during spore formation. As MinCD, DivIVA, and Noc are known to be constitutively expressed[52], their increase in abundance is consistent with inhibition of proteases such as ClpXP and ClpYQ that are responsible for their proteolysis. However, an indirect mechanism cannot be ruled out.

Based on these data, we propose that the increased abundance of the Min and Noc system, two primary systems for inhibition of cell division, contribute to the antibiotic activity of armeniaspirol. A consequence of inhibiting Z-ring function and cytokinesis should be an increase in cells that have two nucleoids. Thus, we examined wildtype *B. subtilis* treated with a sub-lethal dose of **1** (½ MIC). Confocal microscopy of DNA (DAPI) and membrane (FM 4-64FX) stained cells showed statistically significant increase in the number of two nucleoid containing cells in treated versus untreated cells as well as a decrease in single nucleoid containing cells in the treated versus untreated samples (Fig. 5c,d; Supplementary Fig. 3). These observations are fully consistent with our proposed mechanism involving an increase in inhibitors of cell division by blocking ClpYQ and ClpXP protease activity.

Discussion

In this study we have shown that the Gram-positive antibiotic armeniaspirol exhibits a unique antibiotic mechanism of action inhibiting both the ClpYQ and ClpXP proteases. As is seen with many natural products, armeniaspirol has more than one target and exhibits complex pleotropic effects, including dysregulating the divisome of *B. subtilis* via increasing abundance of the Min and nucleoid occlusion systems, two key negative regulators of cell division. A number of antibiotic discovery efforts have investigated inhibitors of the divisome protein FtsZ[53], as inhibition of this highly conserved essential target has been proposed to lead to broad-spectrum antibiotic activity. While potent inhibitors that are active *in vitro* and *in vivo* have been generated, spontaneous mutations of FtsZ leading to

resistance is a serious and potentially limiting concern[54]. In this context armeniaspirol, for which resistance has been undetectable even under laboratory selection conditions[4], appears to be a particularly exciting divisome inhibitor.

While ClpYQ and ClpXP are both AAA+ proteases, they have fundamentally different proteolytic machinery. ClpX is a serine protease with Ser-His-Asp catalytic triad[55]. ClpQ is homologous to the β-subunits of the eukaryotic, archaebacterial, and actinobacterial 20S proteasomes[56]. Uniquely, it possesses an *N*-terminal catalytic Ser rather than *N*-terminal Thr, which is seen in all other 20S proteasomes[21]. The ATPases ClpY and ClpX however are very similar. Both are members of the Clp/HSP100 family[57,58]. ClpYQ is thus a hybrid between the ClpXP-like ATP-dependent proteases and the prokaryotic 20S proteasome. It is therefore somewhat unexpected that armeniaspirol inhibits both ClpYQ and ClpXP. Examination of the amino acid sequence of the protease associated ATPases in *B. subtilis*, *S aureus*, and *E. coli* shows that ClpX and ClpY cluster together and are apart from all other Clp ATPases (Supplementary Fig. 4). This homology, the inhibition of ATPase function (Fig. 4c), and capture of the ClpY ATPase (Fig. 3c) are all consistent with armeniaspirol binding the ATPase subunit, and are thus consistent with inhibition of both ClpXP and ClpYQ by armeniaspirol.

Two additional Clp ATPases, ClpC and ClpE, associate with ClpP and are encoded in the *B. subtilis* genome[59]. As these class 1 Clp/HSP100 ATPases show less sequence similarity to the class 2 ClpX and ClpY ATPases (Supplementary Fig. 5)[58], we propose that ClpC and ClpE are not targeted by armeniaspirol. Consistent with this is the observations that the ClpCP adaptor protein[60] and substrate MecA[61] is decreased in abundance in the armeniaspirol treated proteome and increased in the *ΔclpP* proteome. If ClpCP activity was inhibited by armeniaspirol, it is expected that MecA would increase in abundance as seen in the *ΔclpP* strain. ClpEP activity is likely not inhibited under our experimental conditions since ClpE is expressed only after severe heat shock[62]. Our data thus supports selective targeting of ClpXP and ClpQY over other AAA+ proteases.

A number of natural products are known to target the protease component of AAA+ proteases. These include the 20S proteasomes inhibitors such as epoxomicin[63,64] and related α,β-epoxyketones as well as salinosporamide[65] and similar β-lactone proteasome inhibitors. Both of these families of compounds covalently modify the *N*-terminal catalytic Thr of the 20S proteasome in actinobacteria and eukaryotes[66] but not the ClpQ protease[67]. The acyldepsipeptide (ADEP) natural product antibiotics are known to bind reversibly to ClpP, activating the protease, even in the absence of ATP hydrolysis by the ATPase component[68]. This over activation of ClpP leads to uncontrolled protein degradation and

antibiotic activity[69]. Cyclomarin A, lassomycin, and ecumicin all appear to bind the N-terminal domain of the ClpC ATPase[68]. Cyclomarine A leads to uncontrolled proteolysis[70] where as lassomycin and ecumicin increase ClpCP ATP hydrolysis but inhibits proteolysis[71,72]. Armeniaspirol is highly distinct from all of these. It does not target the protease like the 20S proteasome inhibitors or ADEPS nor does it target ClpCP like cyclomarin A, lassomycin, and ecumicin. Unlike the known ATPase binding natural products, armeniaspirol inhibits ATPase activity and protease activity, suggesting it is targeting a new site on the Clp/HSP100 family. Armeniaspirol represents the first well-characterized ClpYQ inhibitor, and thus may be an exciting starting point for developing novel inhibitors for other ClpYQ proteases, such as the mitochondrial ClpYQ homolog in *Plasmodium falciparum*, whose disruption leads to apoptosis[73].

This study also highlights the pleotropic effects of inhibition of the ClpXP and ClpYQ proteases in *B. subtilis*. The broad physiological effects from inhibition of these two targets, which includes perturbation of the divisome as well as inhibition of DNA replication via GyrB[74] accumulation and peptidoglycan degradation via accumulation of the autolysin LytA (Fig 5b)[75], likely contribute to the lack of observed resistance to the compound. Further deciphering the details of these pleotropic changes will require detailed characterization of the protein targets of ClpXP and the poorly characterized ClpYQ proteases. Armeniaspirol will serve as a powerful pharmacological tool for these studies.

In summary, armeniaspirol has a unique activity targeting ClpYQ and ClpXP proteases, which represent a new bacterial target for antibiotic development. Our results suggest that this unique mode of action is highly robust and we and others[5] were not able to identify resistant strains exposed to sub-lethal exposures to armeniaspirol. Analogs of armeniaspirol have the potential to help overcome the growing public health crisis involving multi-drug resistant organisms.

Acknowledgements

B. subtilis knockout strains MGNA-A784 and MGNA-A086 ordered from National BioResource Project (NIG, Japan): *B. subtilis*. BKE16150 and BKK34540 *B. subtilis* strains were ordered from the Bacillus Genome Stock Centre (BGSC). Expression plasmids harbouring *E. coli clp*X and *clp*P genes were generously provided by Dr. Walid Houry (University of Toronto).

References

1. CDC. Antibiotic use in the United States, 2017: Progress and Opportunities. *US Department of Health and Human Services, CDC,* 1–37 (2017).

2. Brown, E. D. & Wright, G. D. Antibacterial drug discovery in the resistance era. *Nature* **529**, 336–343 (2016).

3. Ling, L. L. *et al.* A new antibiotic kills pathogens without detectable resistance. *Nature* **517**, 455–459 (2015).

4. Dufour, C. *et al.* Isolation and structural elucidation of armeniaspirols A-C: Potent antibiotics against gram-positive pathogens. *Chem. - A Eur. J.* **18**, 16123–16128 (2012).

5. Couturier, C., Bauer, A., Rey, A., Schroif-Dufour, C. & Broenstrup, M. Armeniaspiroles, a new class of antibacterials: antibacterial activities and total synthesis of 5-chloro-Armeniaspirole A. *Bioorg. Med. Chem. Lett.* **22**, 6292–6296 (2012).

6. Sauer, R. T. & Baker, T. A. AAA+ proteases: ATP-fueled machines of protein destruction. *Annu. Rev. Biochem.* **80**, 587–612 (2011).

7. Boersema, P. J., Raijmakers, R., Lemeer, S., Mohammed, S. & Heck, A. J. R. Multiplex peptide stable isotope dimethyl labeling for quantitative proteomics. *Nat. Protoc.* **4**, 484–494 (2009).

8. Michna, R. H., Commichau, F. M., Tödter, D., Zschiedrich, C. P. & Stülke, J. SubtiWiki-A database for the model organism Bacillus subtilis that links pathway, interaction and expression information. *Nucleic Acids Res.* **42**, 692–698 (2014).

9. Bandow, J. E., Brötz, H., Leichert, L. I. O., Labischinski, H. & Hecker, M. Proteomic approach to understanding antibiotic action. *Antimicrob. Agents Chemother.* **47**, 948–55 (2003).

10. Stepanek, J. J., Lukežič, T., Teichert, I., Petković, H. & Bandow, J. E. Dual mechanism of action of the atypical tetracycline chelocardin. *Biochim. Biophys. Acta - Proteins Proteomics* **1864**, 645–654 (2016).

11. Wenzel, M. *et al.* Proteomic signature of fatty acid biosynthesis inhibition available for in vivo mechanism-of-action studies. *Antimicrob. Agents Chemother.* **55**, 2590–2596 (2011).

12. Wenzel, M. *et al.* Proteomic Response of Bacillus subtilis to Lantibiotics Reflects Differences in Interaction with the Cytoplasmic Membrane. *Antimicrob. Agents Chemother.* **56**, 5749–5757 (2012).

13. Freiberg, C., Brunner, N., Macko, L. & Fischer, H. P. Discovering Antibiotic Efficacy Biomarkers. *Mol. Cell. Proteomics* **5**, 2326–2335 (2006).

14. Sender, U., Bandow, J., Engelmann, S., Lindequist, U. & Hecker, M. Proteomic signatures for daunomycin and adriamycin in Bacillus subtilis. *Pharmazie* **59**, 65–70 (2004).

15. Chambert, R., Pereira, Y. & Petit-Glatron, M.-F. Purification and characterization of YfkN, a trifunctional nucleotide phosphoesterase secreted by Bacillus subtilis. *J. Biochem.* **134**, 655–60 (2003).

16. Thomaides, H. B. *et al.* Essential bacterial functions encoded by gene pairs. *J. Bacteriol.* **189**, 591–602 (2007).

17. Peters, J. M. *et al.* A comprehensive, CRISPR-based functional analysis of essential genes in bacteria. *Cell* **165**, 1493–1506 (2016).

18. Sekowska, A. and Danchin, A. The methionine salvage pathway in Bacillus subtilis. *BMC Microbiol.*

2, (2002).

19. Kobayashi, K. *et al.* Essential Bacillus subtilis genes. *Proc. Natl. Acad. Sci.* **100**, 4678–4683 (2003).

20. Kang, M. S. *et al.* The ATP-dependent CodWX (HslVU) protease in Bacillus subtilis is an N-terminal serine protease. *EMBO J.* **20**, 734–42. (2001).

21. Kang, M. S. *et al.* Molecular architecture of the ATP-dependent CodWX protease having an N-terminal serine active site. *EMBO J.* **22**, 2893–2902 (2003).

22. Olivares, A. O., Baker, T. A. & Sauer, R. T. Mechanistic insights into bacterial AAA+ proteases and protein-remodelling machines. *Nat. Rev. Microbiol.* **14**, 33–44 (2016).

23. Rho, S.-H. *et al.* Crystal structure of Bacillus subtilis CodW, a noncanonical HslV-like peptidase with an impaired catalytic apparatus. *Proteins* **71**, 1020–6 (2008).

24. Yu, Y. *et al.* The ClpY-ClpQ protease regulates multicellular development in Bacillus subtilis. *Microbiology* **164**, 848–862 (2018).

25. Yoo, S. J. *et al.* Purification and characterization of the heat shock proteins HslV and HslU that form a new ATP-dependent protease in Escherichia coli. *J. Biol. Chem.* **271**, 14035–14040 (1996).

26. Koo, B. M. *et al.* Construction and Analysis of Two Genome-Scale Deletion Libraries for Bacillus subtilis. *Cell Syst.* **4**, 291–305 (2017).

27. Baker, T. A. & Sauer, R. T. ClpXP, an ATP-powered unfolding and protein-degradation machine. *Biochim. Biophys. Acta - Mol. Cell Res.* **1823**, 15–28 (2012).

28. Keiler, K. C., Waller, P. R. & Sauer, R. T. Role of a peptide tagging system in degradation of proteins synthesized from damaged messenger RNA. *Science* **271**, 990–3 (1996).

29. Gottesman, S., Roche, E., Zhou, Y. & Sauer, R. T. The ClpXP and ClpAP proteases degrade proteins with carboxy-terminal peptide tails added by the SsrA-tagging system. *Genes Dev.* **12**, 1338–47 (1998).

30. Camberg, J. L., Hoskins, J. R. & Wickner, S. ClpXP protease degrades the cytoskeletal protein, FtsZ, and modulates FtsZ polymer dynamics. *Proc. Natl. Acad. Sci.* **106**, 10614–10619 (2009).

31. Camberg, J. L., Hoskins, J. R. & Wickner, S. The Interplay of ClpXP with the Cell Division Machinery in Escherichia coli. *J. Bacteriol.* **193**, 1911–1918 (2011).

32. Camberg, J. L., Viola, M. G., Rea, L., Hoskins, J. R. & Wickner, S. Location of Dual Sites in E. coli FtsZ Important for Degradation by ClpXP; One at the C-Terminus and One in the Disordered Linker. *PLoS One* **9**, e94964 (2014).

33. Gribun, A. *et al.* The ClpP double ring tetradecameric protease exhibits plastic ring-ring interactions, and the N termini of its subunits form flexible loops that are essential for ClpXP and ClpAP complex formation. *J. Biol. Chem.* **280**, 16185–96 (2005).

34. Eymann, C. *et al.* A comprehensive proteome map of growing Bacillus subtilis cells. *Proteomics* **4**, 2849–2876 (2004).

35. Flynn, J. M., Neher, S. B., Kim, Y. I., Sauer, R. T. & Baker, T. A. Proteomic discovery of cellular substrates of the ClpXP protease reveals five classes of ClpX-recognition signals. *Mol. Cell* **11**, 671–83 (2003).

36. Neher, S. B. *et al.* Proteomic profiling of ClpXP substrates after DNA damage reveals extensive instability within SOS regulon. *Mol. Cell* **22**, 193–204 (2006).

37. Feng, J. *et al.* Trapping and Proteomic Identification of Cellular Substrates of the ClpP Protease in *Staphylococcus aureus*. *J. Proteome Res.* **12**, 547–558 (2013).

38. Gerth, U. *et al.* Clp-dependent proteolysis down-regulates central metabolic pathways in glucose-starved Bacillus subtilis. *J. Bacteriol.* **190**, 321–31 (2008).

39. Mi, H., Muruganujan, A., Ebert, D., Huang, X. & Thomas, P. D. PANTHER version 14: More genomes, a new PANTHER GO-slim and improvements in enrichment analysis tools. *Nucleic Acids Res.* **47**, D419–D426 (2019).

40. Belenky, P. *et al.* Bactericidal Antibiotics Induce Toxic Metabolic Perturbations that Lead to Cellular Damage. *Cell Rep.* **13**, 968–980 (2015).

41. Errington, J. & Wu, L. J. Cell Cycle Machinery in Bacillus subtilis. *Subcell. Biochem.* **84**, 67–101 (2017).

42. Levin, P. A., Margolis, P. S., Setlow, P., Losick, R. & Sun, D. Identification of Bacillus subtilis Genes for Septum Placement and Shape Determination. *J. Bacteriol.* **174**, 6717–6728 (1992).

43. Wu, L. J., Errington, J. & William, S. Coordination of Cell Division and Chromosome Segregation by a Nucleoid Occlusion Protein in Bacillus subtilis. *Cell* **117**, 915–925 (2004).

44. Jensen, S. O., Thompson, L. S. & Harry, E. J. Cell Division in Bacillus subtilis: FtsZ and FtsA Association Is Z-Ring Independent, and FtsA Is Required for Efficient Midcell Z-Ring Assembly. *J. Bacteriol.* **187**, 6536–6544 (2005).

45. Gueiros-Filho, F. J. & Losick, R. A widely conserved bacterial cell division protein that promotes assembly of the tubulin-like protein FtsZ. *Genes Dev.* **16**, 2544–2556 (2002).

46. Gündo□du, M. E. *et al.* Large ring polymers align FtsZ polymers for normal septum formation. *EMBO J.* **30**, 617–626 (2011).

47. Levin, P. A., Kurtser, I. G. & Grossman, A. D. Identification and characterization of a negative regulator of FtsZ ring formation in Bacillus subtilis. *Proc. Natl. Acad. Sci.* **96**, 9642–9647 (1999).

48. Tavares, R., Souza, R. F. De, Louzada, G., Meira, S. & Gueiros-filho, F. J. Cytological Characterization of YpsB, a Novel Component of the Bacillus subtilis Divisome. *J. Bacteriol.* **190**, 7096–7107 (2008).

49. Edwards, D. H. & Errington, J. The Bacillus subtilis DivIVA protein targets to the division septum and controls the site specificity of cell division. *Mol. Microbiol.* **24**, 905–915 (1997).

50. van Baarle, S. & Bramkamp, M. The MinCDJ system in Bacillus subtilis prevents minicell formation by promoting divisome disassembly. *PLoS One* **5**, e9850 (2010).

51. Sievers, J., Raether, B., Perego, M. & Errington, J. Characterization of the parB -Like yyaA Gene of Bacillus subtilis. *J. Bacteriol.* **184**, 1102–1111 (2002).

52. Trip, E. N., Veening, J., Stewart, E. J., Errington, J. & Scheffers, D. Balanced transcription of cell division genes in Bacillus subtilis as revealed by single cell analysis. *Environ. Microbiol.* **15**, 3196–3209 (2013).

53. Haranahalli, K., Tong, S. & Ojima, I. Recent advances in the discovery and development of antibacterial agents targeting the cell-division protein FtsZ. *Bioorg. Med. Chem* **24**, 6354–6369 (2016).

54. Stokes, N. R. *et al.* An Improved Small-Molecule Inhibitor of FtsZ with Superior In Vitro Potency, Drug-Like Properties, and In Vivo Efficacy. *Antimicrob. Agents Chemother.* **57**, 317–325 (2013).

55. Lee, B. G. *et al.* Structures of ClpP in complex with acyldepsipeptide antibiotics reveal its activation mechanism. *Nat. Struct. Mol. Biol.* **17**, 471–478 (2010).

56. Bochtler, M., Ditzel, L., Groll, M. & Huber, R. Crystal structure of heat shock locus V (HslV) from Escherichia coli. *Proc. Natl. Acad. Sci. USA* **94**, 6070–6074 (1997).

57. Maurizi, M. R. & Xia, D. Protein binding and disruption by Clp/Hsp100 chaperones. *Structure* **12**, 175–183 (2004).

58. Schirmer, E. C., Glover, J. R., Singer, M. A. & Lindquist, S. HSP100/Clp proteins: a common mechanism explains diverse functions. *Trends Biochem. Sci.* **21**, 289–296 (1996).

59. Elsholz, A. K. W., Birk, M. S., Charpentier, E. & Turgay, K. Functional diversity of AAA+ protease complexes in Bacillus subtilis. *Front. Mol. Biosci.* **4**, 1–15 (2017).

60. Kuhlmann, N. J. & Chien, P. Selective adaptor dependent protein degradation in bacteria. *Curr. Opin. Microbiol.* **36**, 118–127 (2017).

61. Mei, Z. *et al.* Molecular determinants of MecA as a degradation tag for the ClpCP protease. *J. Biol. Chem.* **284**, 34366–34375 (2009).

62. Miethke, M., Hecker, M. & Gerth, U. Involvement of Bacillus subtilis ClpE in CtsR degradation and protein quality control. *J. Bacteriol.* **188**, 4610–4619 (2006).

63. Meng, L. *et al.* Epoxomicin, a potent and selective proteasome inhibitor, exhibits in vivo antiinflammatory activity. *Proc. Natl. Acad. Sci. U. S. A.* **96**, 10403–8 (1999).

64. Groll, M., Kim, K. B., Kairies, N., Huber, R. & Crews, C. M. Crystal Structure of Epoxomicin: 20S Proteasome Reveals a Molecular Basis for Selectivity of α',β'-Epoxyketone Proteasome Inhibitors. *J. Am. Chem. Soc.* **122**, 1237–1238 (2000).

65. Feling, R. H. *et al.* Salinosporamide A: A Highly Cytotoxic Proteasome Inhibitor from a Novel Microbial Source, a Marine Bacterium of the New Genus Salinospora. *Angew. Chemie Int. Ed.* **42**, 355–357 (2003).

66. Borissenko, L. & Groll, M. 20S proteasome and its inhibitors: crystallographic knowledge for drug development. *Chem. Rev.* **107**, 687–717 (2007).

67. Frase, H., Hudak, J. & Lee, I. Identification of the Proteasome Inhibitor MG262 as a Potent ATPDependent Inhibitor of the Salmonella enterica serovar Typhimurium Lon Protease. *Biochemistry* **45**, 8264–8274 (2006).

68. Malik, I. T. & Brötz-Oesterhelt, H. Conformational control of the bacterial Clp protease by natural product antibiotics. *Nat. Prod. Rep.* **34**, 815–831 (2017).

69. Kirstein, J. *et al.* The antibiotic ADEP reprogrammes ClpP, switching it from a regulated to an uncontrolled protease. *EMBO Mol. Med.* **1**, 37–49 (2009).

70. Vasudevan, D., Rao, S. P. S. & Noble, C. G. Structural basis of mycobacterial inhibition by Cyclomarin A. *J. Biol. Chem.* **288**, 30883–30891 (2013).

71. Gavrish, E. *et al.* Lassomycin, a ribosomally synthesized cyclic peptide, kills Mycobacterium tuberculosis by targeting the ATP-dependent protease ClpC1P1P. *Chem. Biol.* **21**, 509–518 (2014).

72. Gao, W. *et al.* The cyclic peptide ecumicin targeting CLpC1 is active against Mycobacterium tuberculosis in vivo. *Antimicrob. Agents Chemother.* **59**, 880–889 (2015).

73. Rathore, S. *et al.* Disruption of a mitochondrial protease machinery in Plasmodium falciparum is an intrinsic signal for parasite cell death. *Cell Death Dis.* **2**, e231 (2011).

74. Samadpour, A. N. & Merrikh, H. DNA gyrase activity regulates DnaA-dependent replication initiation in Bacillus subtilis. *Mol. Microbiol.* **108**, 115–127 (2018).

75. Sanchez-Puelles, J. M. *et al.* Searching for autolysin functions: Characterization of a pneumococcal mutant deleted in the lytA gene. *Eur. J. Biochem.* **158**, 289–293 (1986).

Methods

Cloning and protein purification

B. subtilis clp genes were PCR amplified from *B. subtilis* 168 genomic DNA (Promega Wizard Genomic DNA Purification Kit). The *clp*Q gene was cloned into a pET21 vector (C-terminal His tag, AmpR). The resulting plasmid (pPL29) was transformed into chemically competent *E. coli* BL21(DE3) for protein expression. 400 mL LB media was inoculated with 0.5% (v/v) of an overnight pre-culture. The culture was grown at 37°C (200 rpm) and expression was induced with 1 mM isopropyl-1-thio-β-D-galactopyranoside at an optical density (OD_{600}) of 0.5. The culture was grown at 37°C (200 rpm) for 4 h. The cells were pelleted at 4,000 rpm for 20 min and re-suspended in lysis buffer (50 mM Tris, 100 mM NaCl, 1 µg/mL leupeptin, 1 µg/mL pepstatin A, 1 mg/mL lysozyme, 10% glycerol, pH 8.0). Mechanical cell lysis was achieved by 30 s sonication. The cell debris was pelleted at 10,000 rpm for 60 min and the supernatant was incubated with 800 µL Ni-NTA agarose resin (QIAGEN) for 30 min at 4°C with gentle shaking. The lysate was loaded onto a column and the flow-through was collected. The resin was washed sequentially with 5 mL elution buffer (100 mM Tris, 300 mM NaCl, pH 8.0) containing 0 mM, 20 mM, 100 mM and 250 mM imidazole. Fractions were analyzed by SDS-PAGE (4-20% Mini-PROTEAN TGX Precast Gels; Bio-Rad). Fractions containing purified protein were pooled and buffer exchanged (50 mM Tris, 250 mM NaCl, pH 8.0) using a 10 kDa Amicon Ultra-15 centrifugal filter unit (Millipore Sigma). The concentrated protein was stored at -80°C with 30% (w/w) glycerol. The *B. subtilis clp*Y gene was cloned into pET28b (N-terminal His tag, KanR), and the resulting plasmid (pPL31) was purified as above. All protein concentrations were determined by Bradford assay.

The *E. coli clp*X plasmid (pProEx-Htb-ClpX) was expressed and purified as above in 1 L LB media. The lysis buffer composition included 25 mM Tris, 500 mM NaCl, 1 µg/mL leupeptin, 1 µg/mL pepstatin A, 1 mg/mL lysozyme, 10% glycerol, pH 8.0. The elution buffer composition included 25 mM Tris, 500 mM NaCl, pH 8.0. Fractions containing purified ClpX were pooled and buffer exchanged (50 mM Tris, 200 mM KCl, 25 mM $MgCl_2$, 1 mM DTT, 0.1 mM EDTA, pH 8.0) using a 10 kDa Amicon Ultra-15 centrifugal filter unit. The concentrated protein was incubated with TurboTEV protease (Accelagen) at 1:50 w/w protease:target overnight at 4°C to remove the His tag. 500 µL Ni-NTA agarose resin was added to the mixture for 30 min at 4°C with gentle shaking. The lysate was loaded onto a column and the flow-through was collected. The concentrated untagged protein was analyzed by SDS-PAGE and stored at -80°C with 30% (w/w) glycerol.

The *E. coli clp*P plasmid was expressed as above in 1 L LB media. The cells were pelleted at 4,000 rpm for 20 min and re-suspended in lysis buffer (50 mM Tris, 150 mM KCl, 1 µg/mL leupeptin, 1 µg/mL pepstatin A, 1 mg/mL lysozyme, 10% glycerol, pH 8.0). Mechanical cell lysis was achieved by 60 s sonication. The cell debris was pelleted at 10,000 rpm for 60 min and saturated ammonium sulfate was added to the supernatant slowly with stirring until 40% saturation. Stirring was continued for 60 min at 4°C. The lysate was centrifuged at 10,000 rpm for 30 min and the pellet was discarded. Saturated ammonium sulfate was added further until 60% saturation. Stirring was continued for 60 min at 4°C. The lysate was centrifuged at 10,000 rpm for 30 min and the pellet was discarded. The lysate was buffer exchanged into Buffer A (50 mM Tris, 150 mM KCl, 1 mM DTT, pH 8.0) and filtered through a 0.2 µm syringe filter. The solution was injected onto a 1 mL Q sepharose column (GE Healthcare) and eluted with a linear gradient 0-50% Buffer B (50 mM Tris, 1 M KCl, 1 mM DTT, pH 8.0) over 3 column volumes. 0.2 mL fractions were collected and analyzed by SDS-PAGE. ClpP containing fractions were pooled and buffer exchanged into 50 mM MES, pH 6.0. The solution was injected onto a 1 mL SP sepharose column (GE Healthcare) and eluted with a linear gradient 0-25% Buffer C (50 mM MES, 1 M KCl, pH 6.0) over 25 column volumes. 1

mL fractions were collected and analyzed by SDS-PAGE. ClpP containing fractions were pooled and further purified by size exclusion chromatography (ÄKTA pure 25 M1 FPLC; GE Healthcare) using a Superdex 75 column (GE Healthcare) in 50 mM Tris, 200 mM KCl, pH 8.0. Fractions containing ClpP were concentrated using 10 kDa Amicon Ultra-15 centrifugal filter units (Millipore Sigma). The concentrated protein was stored at -80°C with 30% (w/w) glycerol.

Minimum inhibitory concentrations

MICs were carried out in Mueller-Hinton broth, 100 µL assays in 96-well plates. Sequential concentrations of compound were pipetted into each column through two-fold serial dilutions. 5 µL of bacterial culture (A_{600} 0.07-0.1) was inoculated into each well and incubated at 37°C for 16 h. Growth was observed by A_{600} readings using a Synergy H4 microplate reader (BioTek). The MIC was determined by the lowest concentration of compound that prevented bacterial growth. A *yfkN* CRISPRi knockdown strain was prepared as previously described[17] and subjected to MIC.

Peptide hydrolysis assay

Peptide hydrolysis was assayed using the Cbz-Gly-Gly-Leu-AMC (Millipore Sigma) substrate. 0.1 mL reaction assays were done in 96-well plates. Assays were composed of purified bsClpQ and bsClpY proteins in 0.1 M Tris (pH 8.0), 0.1 mM Cbz-GGL-AMC, 10 mM $MgCl_2$, 1 mM ATP, 1 mM TCEP, and 1 mM EDTA. Peptide hydrolysis for ecClpX and ecClpP was monitored with the substrate Suc-Leu-Tyr-AMC (Millipore Sigma) under the same conditions. A continuous assay of AMC release was monitored at 37°C using a Synergy H4 microplate reader (BioTek) with excitation and emission at 355 nm and 460 nm, respectively. Inhibition was observed with varying concentrations of **1**.

ATP hydrolysis assay

ATP hydrolysis was monitored by a discontinuous assay with a malachite green colour reagent. 3 volumes 0.045% (w/v) malachite green in dH_2O and 1 volume 4.2% (w/v) ammonium molybdate in 4 M HCl were mixed to make the colour reagent. After 20 min of shaking at room temperature in the dark, 100 µL of 2% (w/v) Triton X-100 per 5 mL colour reagent was added, and the resulting solution was filtered through a 0.2 µm syringe filter. Reaction assays contained 10 µM purified bsClpY, 10 µM purified bsClpQ, 1 mM ATP, 10 mM $MgCl_2$, 1 mM TCEP, 1 mM EDTA, 0.1 M Tris (pH 8.0). At specified time intervals, 25 µL of the assay was added to 100 µL of the colour reagent in a 96-well plate. The mixture was incubated at room temperature for 5 min and the absorbance (A_{650}) was read using a Synergy H4 microplate reader (BioTek). Inhibition was observed with varying concentrations of **1**.

Microscopy and image analysis

Biological triplicates of *B. subtilis* 168 was grown in Mueller-Hinton broth with (1 µg/ml) and without compound **1** until an OD_{600} of 0.2-0.25 was reached. 1 mL bacterial culture was prepared on #1.5 coverslips (ThermoFisher Scientific) washed with poly-lysine(K) in phosphate-buffered saline (PBS). The bacterial dilution was fixed with 4% paraformaldehyde-PBS for 10 min at room temperature, and subsequently washed with filter-sterilized 100 mM glycine-PBS for 5 min. The membrane was stained with 5 µg/ml FM 4-64FX (Invitrogen) fluorescent dye while the nucleoid was stained with 2 µg/ml DAPI (Millipore Sigma) fluorescent dye. Coverslips were mounted on Superfrost Plus microscope slides (ThermoFisher Scientific) with Mowiol mounting medium. The slides were left to dry overnight in the dark. Images were obtained with an LSM 880 confocal microscope (Zeiss) using a 100X/1.4 oil immersion objective. Image analysis and cell length measurements were conducted using ZEN Blue (Zeiss) software.

***In vitro* labeling and inhibitor covalent capture**

Fresh *B. subtilis* cell lysate (1 mg/ml) in 100 µL PBS containing 0.05% Triton X-100 buffer was incubated with 80 µM of compound **1** for 1 h, followed by incubation with 10 µM of compound **2** for an additional 1 h. 100 µL of freshly prepared click chemistry mix (100 µM biotin-azide, 2 mM TCEP, 200 µM TBTA, and 2 mM $CuSO_4$) in PBS was added to probe-labeled lysate and incubated for 2 h at room temperature with gentle shaking. The reactions were quenched by addition of 1 mL of acetone and stored at -80 ^oC for at least 30 min. The protein was precipitated by centrifugation at 14,000 rpm for 15 min at 4^oC.The agarose-streptavidin beads (Pierce) were washed three times with 100 µL PBS in a Biospin column. The beads were transferred to probe-labeled cell lysates in 200 µL PBS and incubated for 90 min. For on-bead digestion, the beads were washed five times with 50 mM ammonium bicarbonate, transferred to a 1.5 mL microcentrifuge tube and heated for 15 min at 6^oC in 500 µL of 10 mM DTT in 50 mM ammonium bicarbonate (ABC). After 15 min, 25 µL of 500 mM iodoacetamide was added and lysates were incubated in the dark for 30 min. Samples were centrifuged for 2 min at 1,400 rpm then 100 µL of ABC was added followed by 2 µL of 0.5 mg/mL trypsin. Samples were rotated at 37^oC overnight followed by bead pelleting. The supernatant was collected for LC-MS/MS analysis.

Whole proteome extraction and dimethyl labeling

B. subtilis 168 was grown in 5 mL Mueller-Hinton broth overnight at 37C. The culture was diluted 1/50 in fresh 50 mL Mueller-Hinton broth with (1 µg/ml) or without compound **1** and incubated for 6 hours at 37C (200 rpm). The cells were pelleted at 4,000 rpm for 30 min and re-suspended in 1.25 mL lysis buffer (50 mM Tris, 100 mM NaCl, 1 µg/mL leupeptin, 1 µg/mL pepstatin A, 1 mg/mL lysozyme, pH 8.0). Mechanical cell lysis was achieved by 30 s sonication. The cell debris was pelleted at 10,000 rpm for 10 min. Protein content was quantified by Bradford assay. 50 µg were transferred to a 1.5 mL microcentrifuge tube and the volume was adjusted to 100 µL with 100 mM TEAB buffer. 5 µL of 200 mM TCEP was added to the mixture and incubated at 55C for 1 h. 5 µL of 375 mM iodoacetamide was added and further incubated at room temperature for 30 min in the dark. A methanol/chloroform precipitation was performed to obtain protein pellet. The pellet was re-suspended in 100 µL of 50 mM TEAB buffer containing 0.015% Triton X-100. Protein was digested with trypsin overnight at 37C. A pellet was obtained by vacuum centrifugation and re-suspended with 100 µL of 100 mM TEAB buffer. 4 µL of 4% (v/v) formaldehyde was added to the control reaction, while deuterated formaldehyde was added to **1**-containing reactions. 4 µL of 0.6 M $NaBH_3CN$ was added to all samples and incubated in a fumehood for 1 h with rotation. 16 µL of 1% (v/v) ammonia solution was added to quench the reaction. 8 µL of 5% formic acid (FA) was added and differentially labeled samples were mixed 1:1. All samples were cleaned up with C18 tips (ThermoFisher Scientific) prior to LC-MS/MS analysis.

Mass spectrometry for inhibitor covalent capture

The LC-MS/MS system consisted of an Agilent 1100 micro-HPLC system (Agilent Technologies) coupled with an LTQ-Orbitrap mass spectrometer (ThermoFisher Scientific) equipped with a nano-electrospray interface operated in positive ion mode. A pre-column was packed in-house with reverse phase Magic C18AQ resins (5 µm; 120-Å pore size; Dr. Maisch GmbH), and analytical column of 75 µm × 100 mm was packed with reverse phase Magic C18AQ resins (1.9 µm; 120-Å pore size; Dr. Maisch GmbH). The mobile phases consisted of 0.1% (v/v) FA in water as buffer A and 0.1% (v/v) FA in acetonitrile as buffer B. The sample was loaded onto the pre-column using a buffer containing 98% A at a flow rate of 4 µL/min for 5 min. Subsequently, a gradient from 5% to 35% buffer B was performed, at a flow rate of 0.30 µL/min obtained from splitting a 20 µL/min through a restrictor, in 60 minutes. The MS method consisted of one full MS scan from 350 – 1700 m/z followed by data-dependent MS/MS scan of the 5 most intense ions, with dynamic exclusion repeat count of 2, and repeat duration of 90 seconds. The full MS was performed in the Orbitrap analyzer with R = 60,000 defined at m/z 400, while the MS/MS analysis were

performed in the LTQ. To improve the mass accuracy, all the measurements in Orbitrap mass analyzer were performed with internal recalibration ("Lock Mass"). On the Orbitrap, the charge state rejection function was enabled, with single and "unassigned" charge states rejected.

MS raw files were processed and analyzed using MaxQuant 1.3.0.5. Search parameters were set to allow for N-terminal acetylation, methionine oxidation, and cysteine carbamidomethylation. The enzyme specificity was set to trypsin. A maximum of two missing trypsin cleavages were permitted. The precursor mass tolerance was set at 7 ppm, and 0.8 Da mass tolerance for fragment ions. If the identified peptide sequences of one protein were contained within or equal to another protein's peptide set, the proteins were grouped together and reported as a single protein group. The false discovery rate (FDR) was set to 0.01 for protein identifications. A minimum length of six amino acids was used for peptide identification. Normalized LFQ intensity was used for protein quantification.

Mass spectrometry for dimethyl labeling

The LC-MS/MS system consisted of an Ultimate 3000 nanoRLSC system (Dionex) coupled with an Orbitrap Fusion mass spectrometer (ThermoFisher Scientific) operated in positive ion mode. A 70 µm × 150 mm Luna C18(2) reverse phase column (3 µm; 100-Å pore size; Phenomenex) was packed in-house. The mobile phases consisted of 0.1% (v/v) FA in water as buffer A and 0.1% (v/v) FA in acetonitrile as buffer B. The sample was loaded onto the column using 2% buffer B at a flow rate of 0.30 µL/min for 105 minutes. The method was designed as follows: a gradient from 2% to 38% buffer B was performed for 70 minutes, a gradient from 38% to 98% buffer B for 9 minutes, 98% buffer B for 10 minutes, gradient from 98% to 2% buffer B for 3 minutes, concluded by a 2% buffer B wash for 10 minutes. The Orbitrap Fusion was run in top speed mode and the MS method consisted of a full MS scan from 350 – 2000 m/z with R = 60, 000. Precursor ions were filtered according to monoisotopic precursor selection, +2 to +7 charge state, and 30 seconds ± 10 ppm dynamic exclusion. Fragmentation was performed with collision-induced dissociation (CID) in the linear ion trap. Precursors were isolated using a 2 m/z isolation window, and fragmented with a normalized collision energy of 35%.

Proteome Discoverer 2.1 (ThermoFisher Scientific) was used for protein identification and quantification. The precursor mass tolerance was set at 10 ppm, and 0.6 Da mass tolerance for fragment ions. Search engine SEQUEST-HT implemented in Proteome Discovery was applied for all MS raw files. Search parameters were set to allow for dynamic modification of methionine oxidation, static modification of cysteine carbamidomethylation, and dimethyl modifications on lysine and N-terminus (light and medium labels). The raw files were searched separately with "light" or "medium" labels in the same workflow. The search database consisted of nonredundant *B. subtilis* protein sequences in FASTA file format from the UniProt/SwissProt database. The FDR was set to 0.01, 0.05, and 0.10 for high, medium, and low protein identifications, respectively. Quantification of peptides and proteins was performed using standard settings provided by Proteome Discoverer.

GO analysis

The PANTHER Overrepresentation Test was used to search proteomic data against GO Ontology database (Released 2019-02-02) to identify GO annotations overrepresented in our data when compared to the reference *Bacillus subtilis* genome. Fisher's Exact test with a false discovery rate multiple test correction was used to evaluate the significance.